



Lightweight extensive green roof for building renovation: Summer performance analysis and application in a living laboratory

Graziano Salvalai^{a,*}, Grazia Marrone^a, Marta Maria Sesana^b, Marco Imperadori^a

^a Department of Architecture, Built Environment and Construction Engineering (ABCE), Politecnico di Milano, 20133 Milano, Italy

^b Department of Civil, Environmental, Architectural Engineering and Mathematics, University of Brescia, 25123 Brescia, Italy

ARTICLE INFO

Keywords:

Extensive green roof
Hygrothermal performance
Monitoring
Multi-layer dry construction
Mitigation Strategies
Building renovation

ABSTRACT

Extensive green roofs are considered an effective energy conservation measure for increasing buildings' energy efficiency and reducing the heat wave effect in dense build environments. In this context the present work has a two-fold objective: the first is to test and analyse a commercial extensive lightweight green roof sample through an experimental monitoring campaign carried out in a hot climate during the summer time; the second is to provide a practical case study application showing the architectural integration of the extensive green roof technology for existing buildings. The experimental monitoring campaign has been set for analyzing the temperature levels of an extensive green roof compared with a traditional horizontal roof finished with cement tile. The temperature levels have been analysed through a set of sensors positioned at different levels to characterise the green roof response to the climatic forces during summer. The results show that the air temperature in proximity to the green surface (15 cm above the greenery) is warmer than the undisturbed ambient air temperature during the day and lower during the night by 2–2.5 °C. The soil substrate and the vegetative layer contribute to increase ambient air humidity levels. As expected, the evapotranspiration of the green layer increases during a typical sunny day resulting in more water content in the air above the vegetative level of about 4–8 %. The surface temperature of the ground below the vegetation layer and the temperature of the ground layer (8 cm deep) shows beneficial attenuation and time shift properties with respectively 12–15 °C and 3–4 h. Compared to the traditional cement tiles the green roof shows lower intralayer temperature with differences ranging from 6 to 8 °C. Moreover, the renovation case study represents a practical example of green roof technology integration in a real environment. The study has high replicability, and it is meant to be an interesting example for researchers and professionals to boost the green roof technology application for higher-quality built environments.

1. Introduction

The European goals to reduce carbon emissions are progressively oriented towards renovating urban areas [1]. In the last years, much effort has been put into addressing the overall building's performance, but nowadays, other issues are becoming urgent. Urban Heat Island (UHI), air pollution (AP), human health, and resource scarcity are some of the global environmental issues that need to be addressed [2–5]. Although the ambitious legislation to meet the zero-emission goal has significantly contributed to the overall quality of the European building stock, the European Union also highlights the need for forward-thinking strategies towards the limitation of both the UHI effect's growth and the buildup of excessive pollution concentration. The EU is going to revise

the 2008/50/EC directive on ambient air quality and cleaner air for Europe [6] proposing stricter air quality regulations inside and outside the buildings. In this context, the use of mitigation strategies to influence internal and external environmental conditions and to improve the cities' air quality has become a priority. In recent years, the scientific community focused on studying Nature Based Solutions (NBS), given their tendency to draw on natural processes offering multiple co-benefits and enhancing or conserving nature, thus representing a carbon-neutral strategy [7]. Various approaches have been proposed to integrate NBS into the building envelope. Among others, significant attention has been paid to the potential of green roofs to reduce the energy stored in urban horizontal surfaces [8] and contribute to air quality improvement [9,10] by fixing air pollutants [11] and reducing the UHI [12]. Green roofs are

* Corresponding author at: Architecture, Built environment and Construction department, Via Ponzio 31 20133 Milan, Italy.

E-mail address: graziano.salvalai@polimi.it (G. Salvalai).

available in a wide range of solutions and can be considered multi-functional systems. They contribute to the assessment of different performances, such as thermal [13], hydraulic [14], and acoustic [15], also considering different types of substrates and vegetation [16]. As NBS, green roofs can improve the stormwater retaining capacity and urban air quality and increase the overall energy efficiency of buildings towards zero carbon emission target [17]. Moreover, the development of green roofs as industrialised multi-layer systems can increase their application range. However, the existing literature on the topic merely addresses microclimatic and thermophysical processes as one-way sectorial disciplines without considering the system's multiple benefits [18]. On one side, there are scientists focused on mathematical modelling [19] and simulation [20] of the physical phenomena influencing the thermal performances of green roofs. On the other side, experimental investigations are conducted comparing different roof construction systems [21,22]. Since a green roof is composed of different layers, its behaviour is influenced by several parameters, from external climatic conditions [23] to physical phenomena [24]. The type of green roof, its geometrical properties, soil depth, moisture content, density, thermal diffusivity, and vegetation choice can contribute to the system's overall performance [25]. Considering the required level of maintenance, which varies with the depth of the soil substrate layer [26], the literature agrees with classifying green roofs as intensive, semi-intensive and extensive [27,28]. The extensive green roof typically consists of low-maintenance greenery with very high drought resistance and a lightweight substrate (i.e., a soil layer thickness of less than 20 cm and saturated weight of less than 150 kg/m² [29]), allowing its installation on existing roofs with limited structural load-bearing capacity. Accordingly, extensive green roofs show great potential in retrofitting interventions. The semi-intensive and intensive green roofs allow articulated modelling of the surface and the use of a wide range of species thanks to the depth of the substrate layer (i.e., a soil layer thickness of more than 20 cm, saturated weight of more than 200 kg/m²). Usually, intensive green roofs are designed for complete accessibility and applied to new buildings since the weight has to be considered in the building's structural design [27]. Generally, extensive green roofs are equipped with self-sustaining plant species which require low irrigation and can survive water runoff more effectively [30] thus, they appear beneficial in dry and hot seasons [31]. They supply building energy savings mainly through the substrate evapotranspiration process, essential for releasing cooling effects [32–34] and reducing the cooling load of buildings [34,35], the VOC mixture and contributing to the CO₂ sequestration [36]. Contrariwise, intensive green roofs show low performance in saving cooling energy due to the limited biodiversity. Moreover, the substrate thickness has a high moisture-holding capacity which generates a green-roof heat-sink effect showing better performance in cold climate areas [37]. Various approaches have been investigated to highlight the use of green roofs as a tool for a mitigation strategy at both urban and building scales. Many empirical [38,39] and theoretical studies have been published to address [40] and compare [41] the performance of multi-layer green roofs, which combine the water retention layer, substrate, and various vegetation types [42]. The presence of vegetation and water bodies can effectively influence thermal energy [31] performances mitigating the UHI effect according to (i) the contribution of the vegetation layer, varying on the type of plants used and improving environmental quality by controlling emissions of Volatile Organic Compounds (VOC), (ii) the substrate depth, reducing energy consumption, (iii) the substrate water content and storage of rainfall water, preventing runoff events, (iv) the thermal resistance value of the substrate, which can significantly influence the thermal behaviour, and (v) the type of drainage system used according to the application contexts and building technology. The green roof temperature fluctuations as well as rainfall runoff were attained compared to the traditional roof systems [37–39].

Besides the benefits of green roofs in energy savings, recent years have seen an increasing interest in their microclimate and hygrothermal

properties' contributions [43]. However, further research is needed to address lightweight extensive green roof systems's hygrothermal properties in summer conditions also investigating their potential to boost building renovation interventions. Moreover, the variety of green roof systems available on the market pinpoints the need to provide reliable data and knowledge of their hygrothermal properties. This work contributes to the identified research gaps by providing data about the summer hygrothermal performances of a lightweight extensive green roof, also offering a comparison with a cement tile to provide benchmark values of surface and interlayer temperatures according to the variations of the external climatic conditions. Moreover, through a case study application, the research is enriched by the installation of a lightweight extensive green roof on a test facility building in a temperate climate. The case study has been described in detail to bridge the gap between research and real-world application.

The work is structured into four main sections: after the introduction, section 2 describes the experimental set-up and monitoring campaign conducted to collect the data and the technical description of the case study building before the renovation intervention. Section 3 shows through several graphs the experimental results and the authors' interpretation and section 4 shows the architectural green roof integration in a living laboratory as a practical example of building renovation. The paper closes with a discussion of the findings, including limitations and suggestions for future research.

2. Methods of work and experimental set-up

Green roofs have proven to be a ready and affordable technological solution able to mitigate peak temperatures in dense urban areas contributing also in reducing the energy consumption of buildings and providing thermal protection mainly during the hot summer season. Starting from this, the present study focuses primarily on the analysis of the summer performance of the green roof technology comparing the temperature level with a common horizontal roof finishing. The methodology reported in this section is presented according to the two main objectives of this study: i) preliminary experimental monitoring campaign in a hot climate during summer climate conditions and ii) study and detailed description of a practical case study green roof application in a living laboratory located in Milan, Italy. The first part of the methodology describes the set-up of the monitoring campaign conducted to assess the summer hygrothermal performances of the extensive green roof. Hygrothermal performances of the green roof sample have been measured on a building's roof close to the living laboratory as a representative case of the operating conditions. The results have been compared with typical cement tile finishing, traditionally used for flat roof claddings, to provide a reference point.

2.1. Experimental set-up and sensor implementation

The hygrothermal performance analysis of the lightweight extensive green roof has been carried out using a detailed monitoring system. The experimental campaign was carried out in July 2019 to assess and compare with traditional roof coating systems, the performances of the green roof technology under summer climate conditions. The experiment was conducted through a certified monitoring system for 13 days, from 12th July 2019 at noon to 25th July 2019 at 6 PM. The monitoring set-up has been set for collecting both the temperature level of the green roof sample and the typical horizontal roof technology covered by pre-fabricated cement tiles, traditionally used for the roof coating. The cement tile is approximately 40x40 cm in size and 2.5 cm thick, it is separated from the roof's structure by 1 cm air cavity; a bituminous membrane protects from water infiltration from the structural layer below. The tested green roof technology has been developed for rooftop applications for new and renovated buildings. The system is characterized by limited weight and thickness: the depth is approximately 13,0 cm, while the weight measured during maximum saturation equals

93,00 kg/m², the total water content of 30,50 l/m² and the air volume is equal to 46,50 l/m². Four main layers compose the overall roof system, from top to bottom: 1) Vegetation layer (Mixture of Sedum), 2) roof soil substrate, 8 cm thick, 3) small flow element filter membrane, 4) component for drainage and water storage in expanded polystyrene. The analyzed green roof sample has a dimension of 80x60 (l × w) cm with the perimeter of the box made by a thin steel grid to maximize the green surface; the monitoring sensors have been positioned in the middle of the sample to minimize the boundary effect. According to the existing literature [33], the sample set-up is suitable for the thermo-hygrometric green roof analysis. Fig. 1 shows the schematic design of the two roofs tested.

The monitoring equipment consisted of a certified data logger set connected to temperature, relative humidity (RH), and solar radiation sensors. A scheme of the sensor's placement is represented in Fig. 1, while a detailed description of the sensors is reported in Table 1. The data has been collected with a granularity of 15 min further aggregated hour by hour [44].

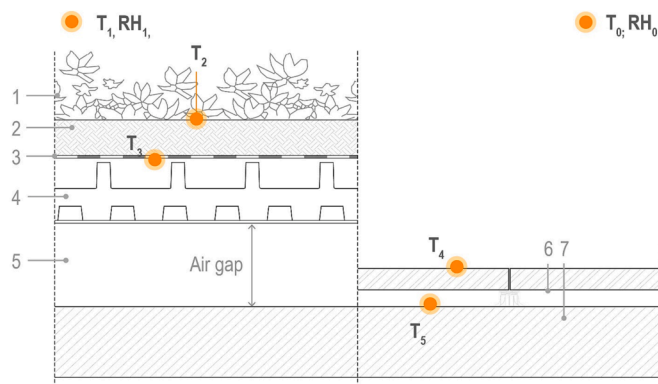
2.2. The living laboratory building

The test facility building object of the intervention is located at the Bovisa Campus of Politecnico di Milano University, in a Nord-West suburban area of Milan (Italy). It is an example of the reuse and renovation of the model home for the Mediterranean climate named Atika [45]. After the renovation, the building changed its name to VELUXlab and turned into a test facility building equipped with innovative building materials and sensors. The building responds to the changing internal and external conditions by smartly and actively adjusting itself to reach indoor comfort. Only in the extreme season, it needs help from the mechanical system of acclimatization and ventilation. The building was assembled using semi-volumetric prefabricated portions and was completed with the multi-layer dry construction technique [46]. The building envelope is hyper-insulated, with excellent winter and summer performance. The main steel structure is completed with lightweight

Table 1

Technical description of the experimental measurement equipment.

Sensor/logger type	Sensor/logger technical specifications
Hobo data logger Rx3000 type	Represents the central unit to collect and process data. Each sensor which measures physical quantities is connected to the data logger. This instrument provides the storage of the collected data in an online server. It sends the data to the server every 5 min. All the data are accessible via the web;
Surface temperature sensor (Onset S-TMB-M006 sensor)	Consists of a small thermocouple assembled on a metal element and connected to the surface of the sample by a conductive adhesive paste. It can be thermally insulated to the outside with insulating material. Measurement Range: -40° to 100° °C Accuracy: $< \pm 0.2^{\circ}$ °C from 0° to 50° °C Resolution: $< 0.03^{\circ}$ °C from 0° to 50° °C
Air and humidity sensor (Onset S-THB-M002 Sensor)	Consists of a sensor (Platinum100) to measure temperature and a capacitive sensor to measure relative humidity. When used in an outdoor environment it is protected by a special anti-radiation screen. Measurement Range: Temp: -40° °C to 75° °C, RH: 0–100 % RH at -40° to 75° °C Accuracy: Temp: $\pm 0.21^{\circ}$ °C from 0° to 50° °C, RH: ± 2.5 % from 10 % to 90 % RH Resolution: Temp: 0.02° °C at 25° °C, RH: 0.1 %
Solar radiation - Pyranometer sensors (Onset S-LIB-M003)	The Pyranometer is a thermopile sensor to measure global solar radiation. It measures the diffuse component of sunlight in the spectrum of $0.3 \mu\text{m} \div 3 \mu\text{m}$ with a range from 0 to 2000 W/m ² . Measurement range: 0 to 1280 W/m ² . Operating temperature range: -40° to 75° °C. Accuracy: ± 10 W/m ² or ± 5 % Resolution: 1.25 W/m ²



1. Sedum, herbaceous perennial ground cover plants;
2. Volcanic aggregate mix with water retention capacity $\geq 40\%$, available water $\geq 30\%$, 8 cm settled;
3. Stabilising geotextile in polypropylene fibres, raw mass 220 gr/m², 1.35 mm;
4. Drainage and water storage element in expanded polystyrene, raw mass 25 kg/m³, thickness 47 mm;
5. Air gap of 60 cm;
6. Cement tile, thickness 20 mm;
7. Black bituminous membrane, thickness 4 mm.

● Sensor's placement

T_0, RH_0 : Ambient air temperature and RH; T_1, RH_1 : Temperature and RH 15 cm above the vegetation layer; T_2 : Surface temperature ground substrate; T_3 : Interlayer ground substrate temperature; T_4 : Cement tile's surface temperature; T_5 : Temperature under cement tile.



Fig. 1. Schematic representation of sensor's location within the two samples and images of the experimental setup.

steel frames, while the floor is a hybrid structure of galvanized metal sheets and reinforced concrete. The façade is isolated with mineral wool, wood wool and polyurethane, with recycled glass fibre cladding. The roof can be considered the main façade of the building enhancing natural ventilation through its tilted shape. Before the renovation intervention proposed in this study, the original building's roof was isolated with 60 mm of polyurethane with a ventilated gap, under it 75 mm of wood wool and 80 mm of rock wool and completed with raw aluminium slats resulting in a ventilated and thermoreflexive roof. To increase the sustainability of the building and test the potential heat mitigation effect of green roofs, some portions of the actual roof have been integrated with the studied green system. This has led to verifying the practical architectural integration in a real environment highlighting the high replicability of the practice.

3. Experimental monitoring campaign results

The present section reports on the performance study of the light-weight extensive green roof and focuses on comparing the temperature level of the different material layers with a traditional roof finishing. The section is composed of three main subsections: [Section 3.1.](#) describes the microclimate condition during the monitoring campaign, [Section 3.2](#) compares the temperature levels of the superficial layer of the two samples, and [Section 3.3](#) compares the temperature levels behind the two roof finishing technologies.

3.1. Microclimate conditions during the monitoring campaign

The experimental monitoring campaign lasted for 13 days, from 12th July at noon and ended on 25th July at 6 PM. The external climatic conditions during the monitoring campaign are reported [Fig. 2](#) in [Fig. 3](#) and [Fig. 4](#).

The prevailing general daily weather condition is indicated by symbols on the top of the charts to allow an easier data reading. [Fig. 3](#) highlights the values of the ambient air temperature and relative humidity while [Fig. 4](#) reports the relationship between ambient air temperature and global solar radiation over the 13-day monitoring period.

As shown by the graphs the weather conditions during the experimental monitoring campaign were characterized by a prevalent clear sky with ambient air temperature peaks over 30 °C with a peak-to-valley amplitude between 12 and 15 °C during the hottest days. One typical summer rain event was registered between July 14th and July 16th, the rest of the monitoring campaign was characterized by hot and sunny days with air temperature peaks above 35 °C and horizontal global radiation higher than 800 W/m².



Fig. 2. Test facility building' aerial views before the green roof renovation intervention. (For interpretation of the references to colour in this figure legend, the reader is referred to the web version of this article.)

3.2. Measurements of the surface temperature levels of the vegetative layer and cement tile

In this paragraph, the substrate surface temperatures of the green roof sample are presented and compared to the values gathered from the surface temperatures of the cement tile roof coating. [Fig. 5](#) shows that the cement tile's surface temperature is always higher than the substrate's, showing deviations between 5 and 14 °C according to the weather conditions and the water soil content.

The measurement reported in [Fig. 6](#) highlights the effect of the water content on the measured surface temperature. During the rainy day (15/07/2019), the green roof substrate increases the water content (the technology has a normal water capacity of 30 l/m²) allowing a lower surface temperature of the green substrate for the next days.

In detail, the temperature difference between the green surface and the cement finishing registered on July 14th is about 10 °C with the temperature of the cement tile 21 °C higher than the air temperature. After a rain event, the temperature level of both samples has drastically reduced, with the temperature of the vegetative layer reaching the same level as the air ambient temperature. The temperature profile of the concrete finishing is still significantly higher with a difference of up to 6 °C during the central hour of the day. [Fig. 7](#) reports the temperature behaviour during and after a series of hot and sunny days. The surface temperature profile is comparable with lower differences mainly concentrated in the peak and the valley of the curves profile. The maximum temperature peak of the green layer is 3–4 °C lower than the concrete finishing.

[Fig. 8](#) showcases two thermal camera pictures, taken on 24th July at 10.25 a.m., for verifying the overall temperature level of the two samples. The thermal imaging camera T620 with a sensor resolution of 640x480 and 307,200 pixels has been used. The emissivity value of the construction material represents a critical parameter in processing the infrared picture. The values normally vary between different materials with a significant impact on the surface temperature level. Regarding the tested materials, the following properties have been considered: (i) cement tiles (light grey): albedo 0,5 and emissivity 0,9; (ii) green roof substrate: albedo 0,32 and emissivity 0,95.

The infrared images offer an intuitive representation of the surface temperature difference between the vegetation layer and the exposed surface of the cement tile. To have a comprehensive overview of the data gathered with the thermal camera, also the temperature profiles are reported in [Fig. 8](#). As shown, the surface temperature of the greenery is less homogenous than the tile surface temperature and presents in general as an average value temperature lower by 6–10 °C concerning the concrete tile surface (picture on the right side). In terms of relative humidity [Fig. 9](#) reports the comparison between the ambient air relative



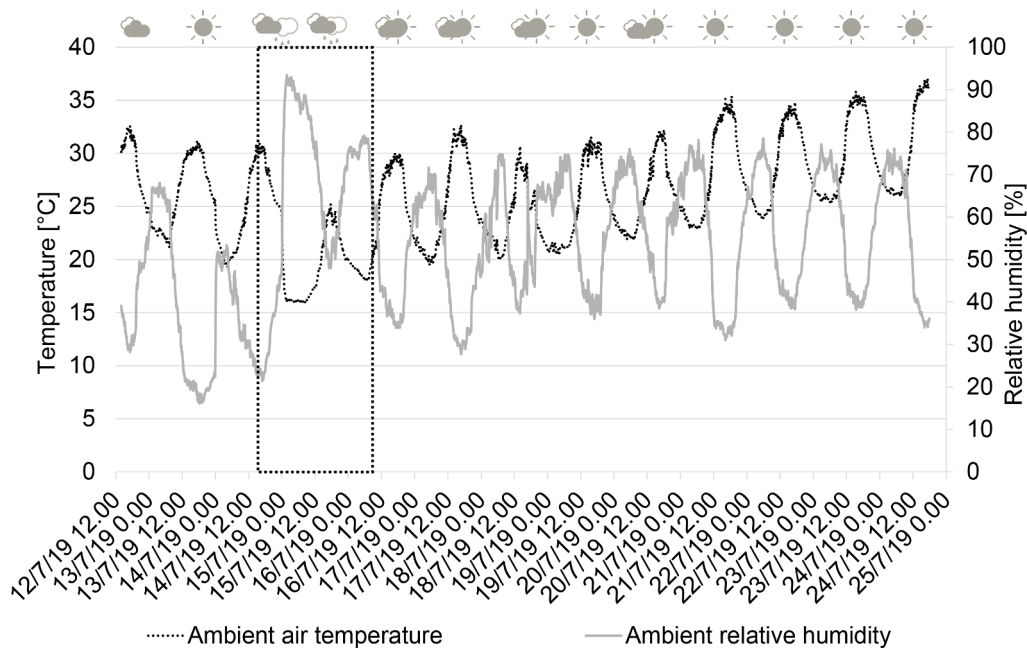


Fig. 3. Ambient air temperature and relative humidity measured during the monitoring campaign.

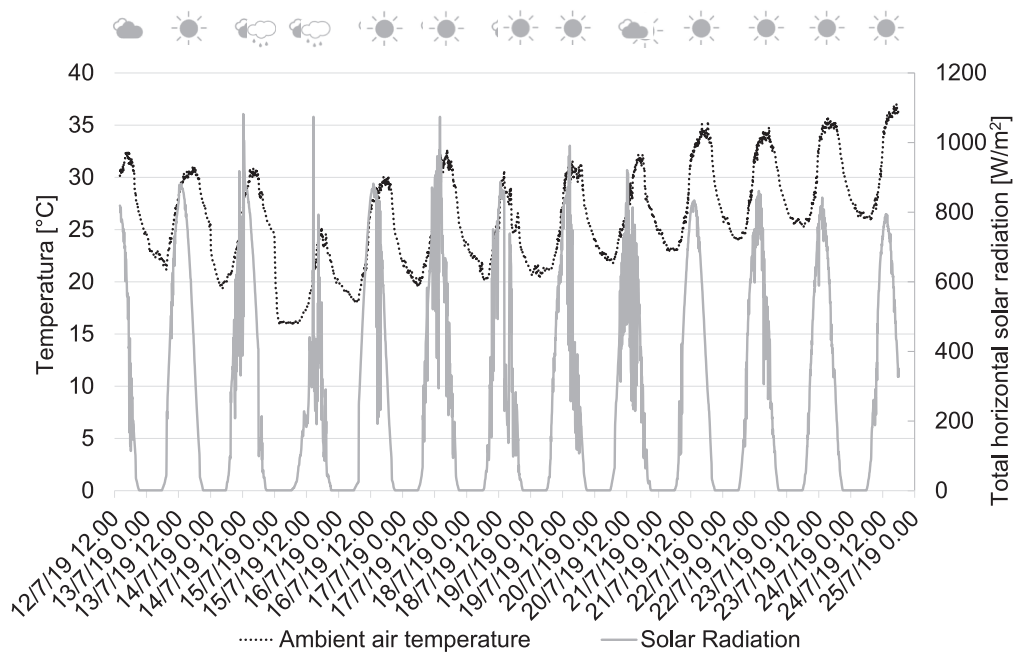


Fig. 4. Ambient air temperature and global solar horizontal radiation measured during the monitoring campaign.

humidity measured respectively above the green roof substrate and the one measured over the cement tiles finishing. In general, the two humidity levels do not show a high difference between each other. The air humidity above the two surfaces has been measured through two capacitive RH sensors. As expected, during a rainy day, the soil contributes to an increase in the related air humidity values due to the water content of the soil/vegetative layer.

Fig. 10 shows a detailed picture of typical summer days characterized by high solar radiation and air temperature. As expected, the evapotranspiration process of the green layer increases during the days resulting in more water content in the air above the vegetative layer of about 4–8 %. During the nighttime, the air humidity level is comparable with the minimal difference between the two measured points. The

experimental data demonstrate that the air temperature is the primary driver of the evaporation process, but other factors also play a role such as the humidity level; moreover, the evaporation rates decrease with increasing humidity with all other factors kept constant [47].

3.3. Measurements of the interlayer temperatures (ground layer vs under tile)

This section reports the results gathered by comparing the interlayer temperature of the green roof substrate (at 8 cm below the vegetation layer) to the temperature gathered under the cement tile of the reference roof system. Fig. 11 shows the measured surface temperature profile together with the air ambient temperature. The label reported

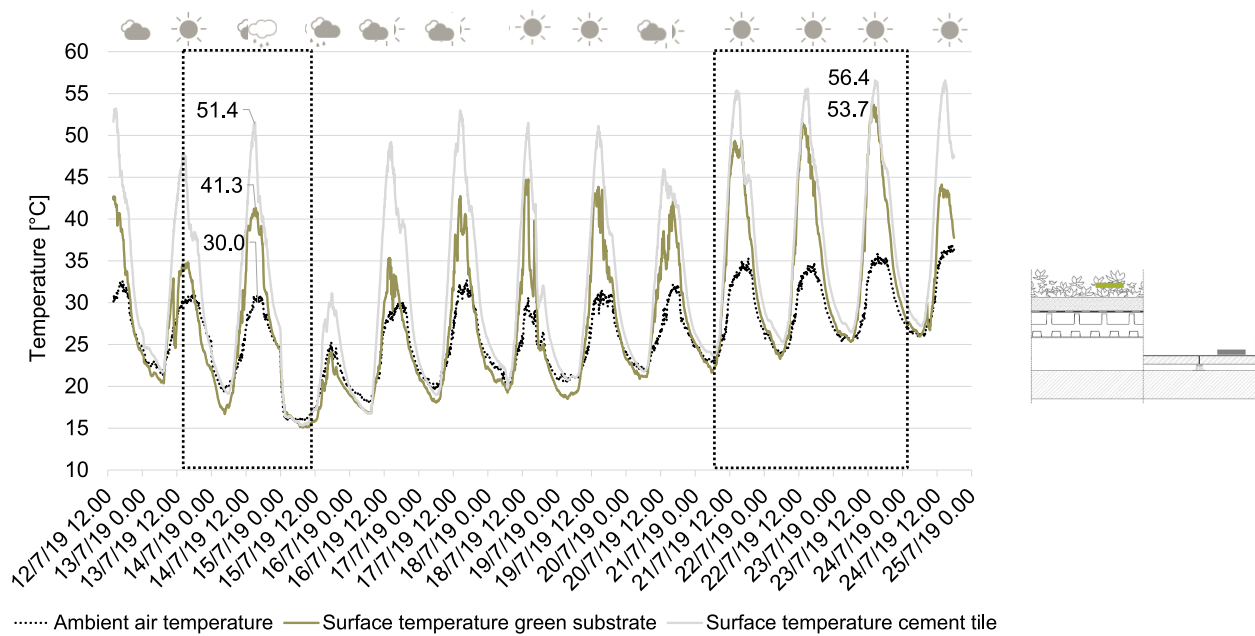


Fig. 5. Comparison between the green roof and the cement tile's surface temperatures. (For interpretation of the references to colour in this figure legend, the reader is referred to the web version of this article.)

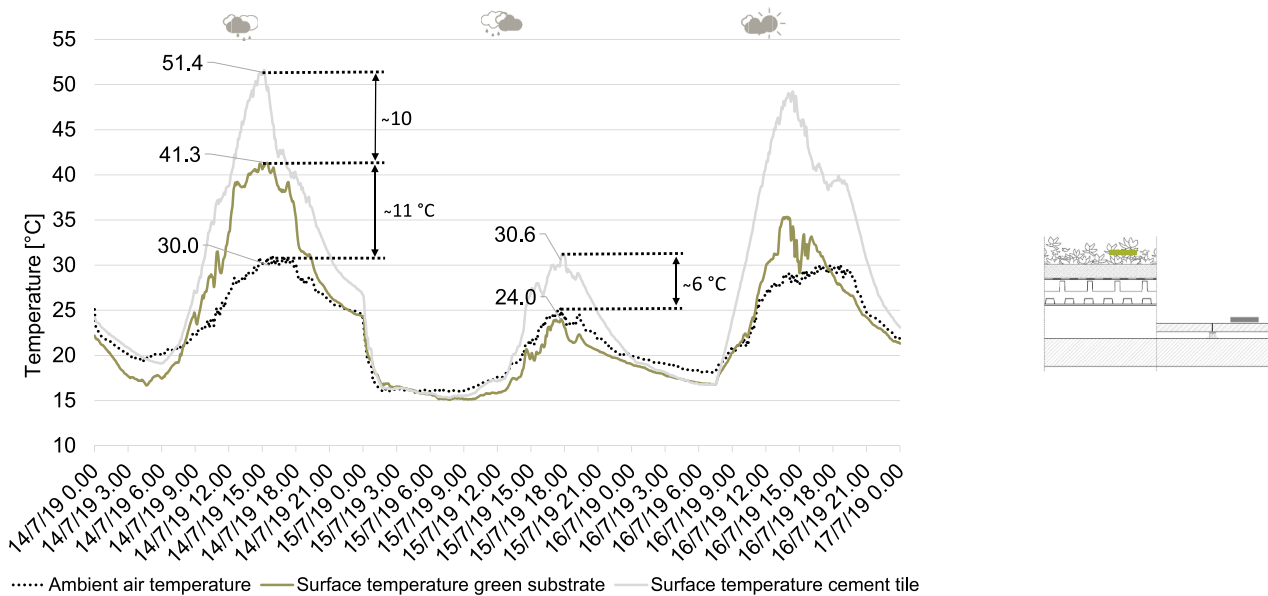


Fig. 6. Measurements of the surface temperatures for three days period between the 14th and 16th of July 2019.

highlighting the difference between the two measured points under two different weather conditions: a rainy day and a typical summer day.

In general, the ground substrate's intralayer offers a consistent mitigation effect with a significantly lower temperature than one below the traditional cement tile finishing. On average, the temperature registered under the cement tile is 5–7 °C higher than the substrate's intralayer temperature. The following figures highlight two specific time frames of the monitoring campaign. Fig. 12 reports the temperature level registered during the 15th of July (rainy day) and Fig. 13 reports the temperature profile collected during the typical sunny day (17th of July). In the case of rain and cloudy sky, the thermal shift provided by the green roof is equal to 3.5 h with a temperature attenuation of 8 °C concerning the temperature registered below the tile finishing. Moreover, the presence of the soil water influences the overall thermal

behaviour during the following day.

Fig. 13 shows the temperature profile during a series of typical summer sunny days. From the chart is evident a series of homogenous sinusoidal waves characterized by 4 h time shift of and up to 9 °C attenuation capacity. From the results, the green roof technologies show high potential in mitigating the thermal flux from inside the building and the beneficial effect on the external built environment. Fig. 14 highlights the temperature profile calculated as a difference between the soil level and the surface layer behind the cement tiles. As expected during rainy days the temperature difference decreases reaching parity and increases again the day after with high global solar radiation. In general, the monitoring shows a maximum temperature difference that ranges from 10 to 13 °C during the day and between 0 °C and 4 °C during the night.

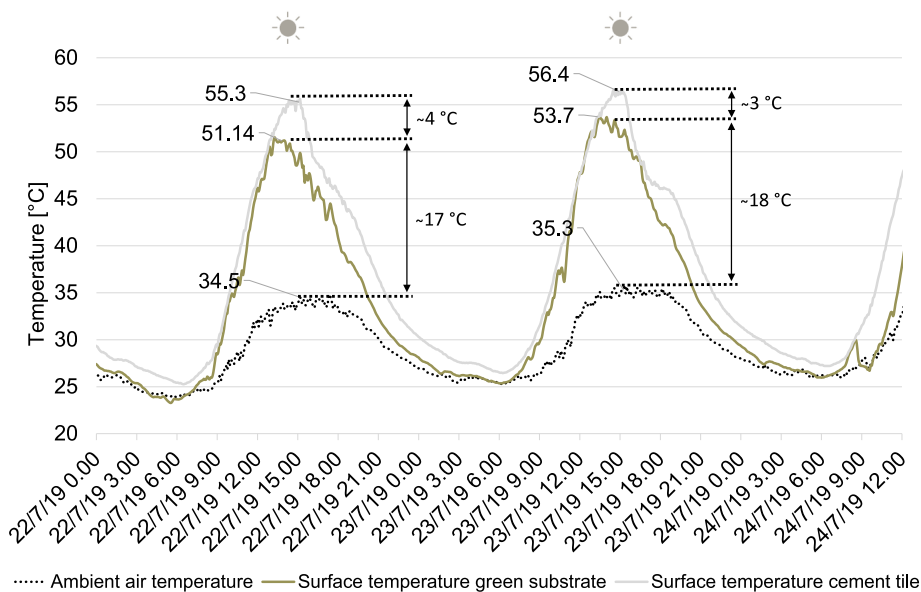


Fig. 7. Measurements of the surface temperatures for three days period between the 22nd and the 23rd of July 2019.

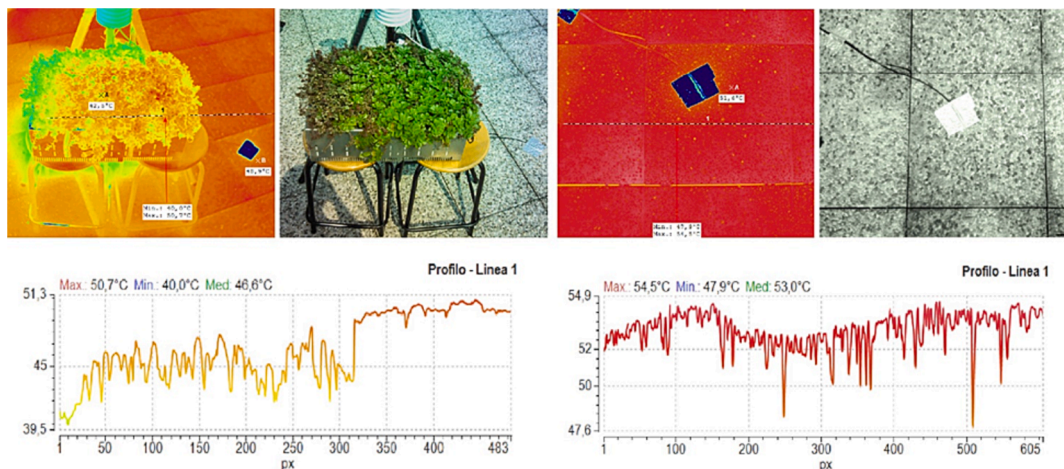


Fig. 8. Infrared pictures of the two samples and related profiles of the surface temperatures (24th July).

Fig. 15 shows the distribution of the intralayer soil temperatures and temperatures under the cement tiles as a function of the ambient air temperature. As expected, the soil intralayer temperatures show a lower temperature fluctuation during the whole day, with the highest variation ranging from 10 to 11 °C. The temperatures registered below the cement tile finishing show in general a lower temperature stability with a max temperature difference of up to 20 °C.

The thermal inertia offered by the soil together with the water content mitigate the solar radiation effect with beneficial impact both to the inner and outer spaces. Fig. 16 reports the scatter plot of the vegetative layer and the external surface of the cement tile versus the ambient air temperature. The temperature distribution is more homogeneous with a closed R^2 value. As shown in the figure the surface temperature of the cement tile presents a temperature level shifted by 7 °C when the ambient air temperature is between 28 and 32 °C.

4. Green roof technology application in a living laboratory

The case study application is presented and discussed in this section to illustrate the feasibility of lightweight green roof technology for building renovation. The case study has been presented in section 2.1 as

an interesting living laboratory where researchers and students can apply and test different building envelope components. In 2020 the test facility building's roof was renovated using the green roof technology presented in the previous sections for covering 28 m² of the existing roof characterized by a multi-layer dry assembled technology as presented in Fig. 17.

The renovation intervention took place between 18th March and 2nd April 2020. The authors identified three main steps to carry out the renovation intervention: (i) removal of the original external cladding (raw aluminium staves, transpiring and waterproof membrane and wooden slats), (ii) placement of the sandwich panel layer and (iii) placement of the lightweight green roof system. Fig. 18 reports three pictures representing the main phase of the existing finishing removal.

The extensive green roof has been integrated with a bilayer metal-faced sandwich panel. The sandwich panel, on the one hand, offers thermal insulation and, on the other hand, works as a load-distributing layer for the green roof system. Moreover, the upper metal sheet of the sandwich panel is preassembled with a PVC waterproof membrane to increase the durability of the overall system. To protect the oriented straight board layer, a new waterproof and breathable membrane has been installed and taped before the installation of the sandwich panels.

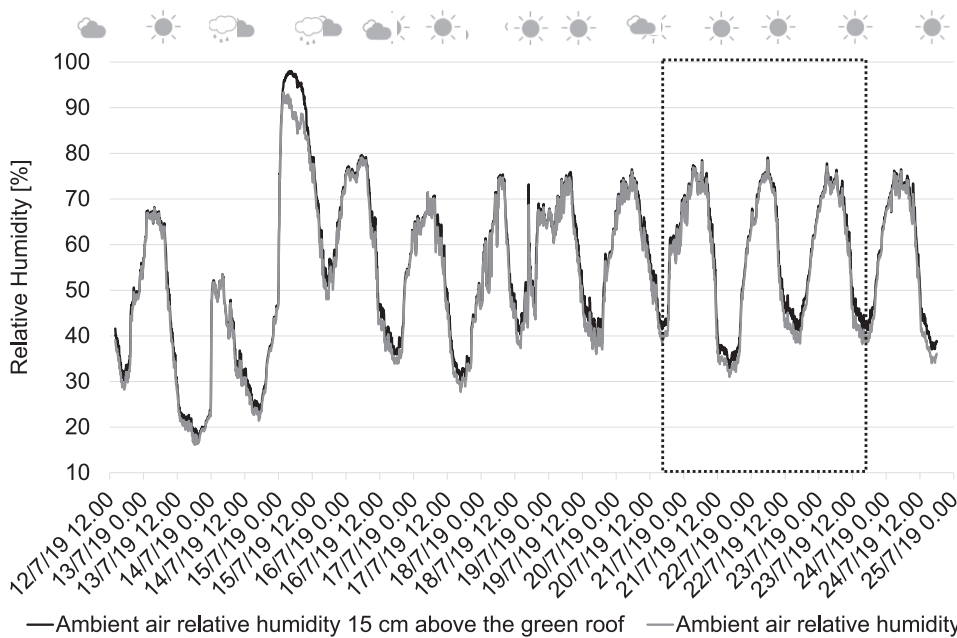


Fig. 9. Full test measurement data of the ambient air relative humidity measured above the green substrate and the cement tiles. The data refers to the whole monitoring campaign.

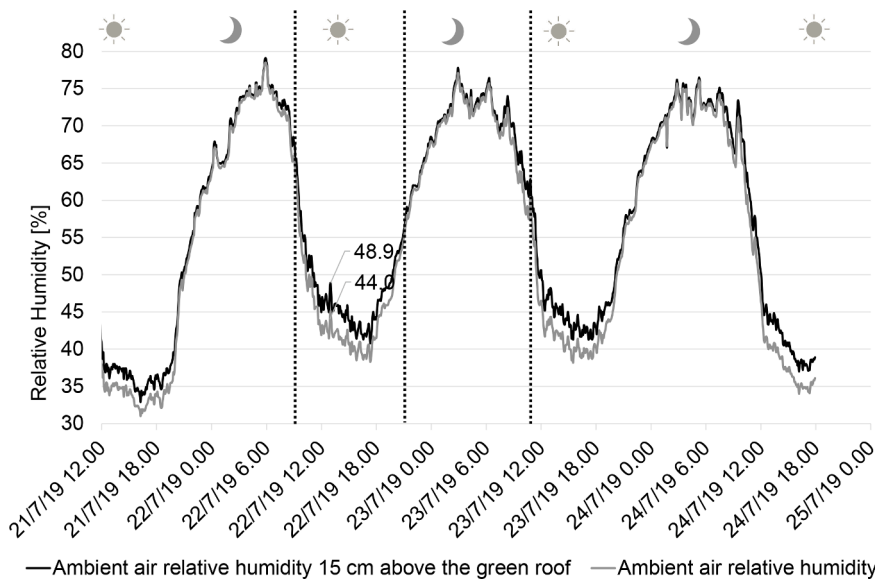


Fig. 10. Detail of the measured ambient air relative humidity for three days (22nd – 25th of July). The chart compares the relative humidity level measured above the green substrate and the relative air humidity above the cement tiles.

Fig. 19 shows the new roof layering and Fig. 20 collects some representative pictures of the main renovation phases.

Afterwards, the placement of 40 mm thick sandwich panels insulated with polyurethane fastened to the light steel frame substructure took place. The panels' fixing to the substructure occurs mechanically with screws and special sealing caps, thus weakening the synthetic membrane pre-bonded offsite to the sandwich panels. To prevent water infiltration between one panel and the other, a PVC-P pontage band is applied and welded to the sandwich panel's pre-bonded membrane. The last phase involves the installation of the extensive green roof, which starts with placing a waterproof and root barrier membrane on the installed sandwich panels. Secondly, the drainage and water retention layer has been installed, placing a stabilising geotextile above it to separate the drainage system and the substrate above. Before the soil is placed on the

lightweight green roof system, it is necessary to place a soil retention system made of polyethene geocells to avoid the soil sliding due to the pitching of the roof. In conclusion, the renovation process of the test facility building's roof was completed in 14 working days with an installation of 2 m² of new green roof per day.

5. Discussion and limitations of the study

The outcomes of this research have provided insights into the hygrothermal performances of an extensive and lightweight green roof technology in a real environment during the summer season, enriching the results with a real case study application of the technology in the renovation of a living laboratory. However, the results should be interpreted considering the limitations of the current research. In this

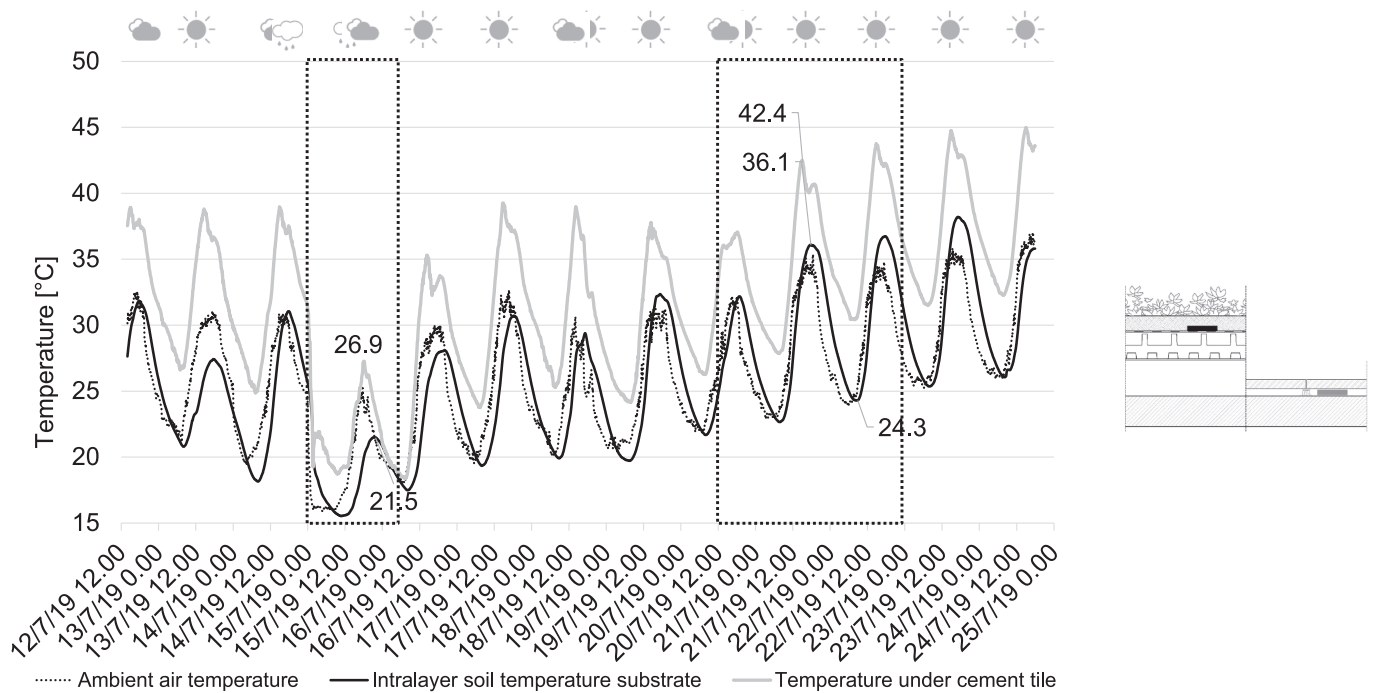


Fig. 11. Comparison of the substrate’s intralayer temperatures and the temperatures under the cement tile. The data refers to the whole monitoring campaign.

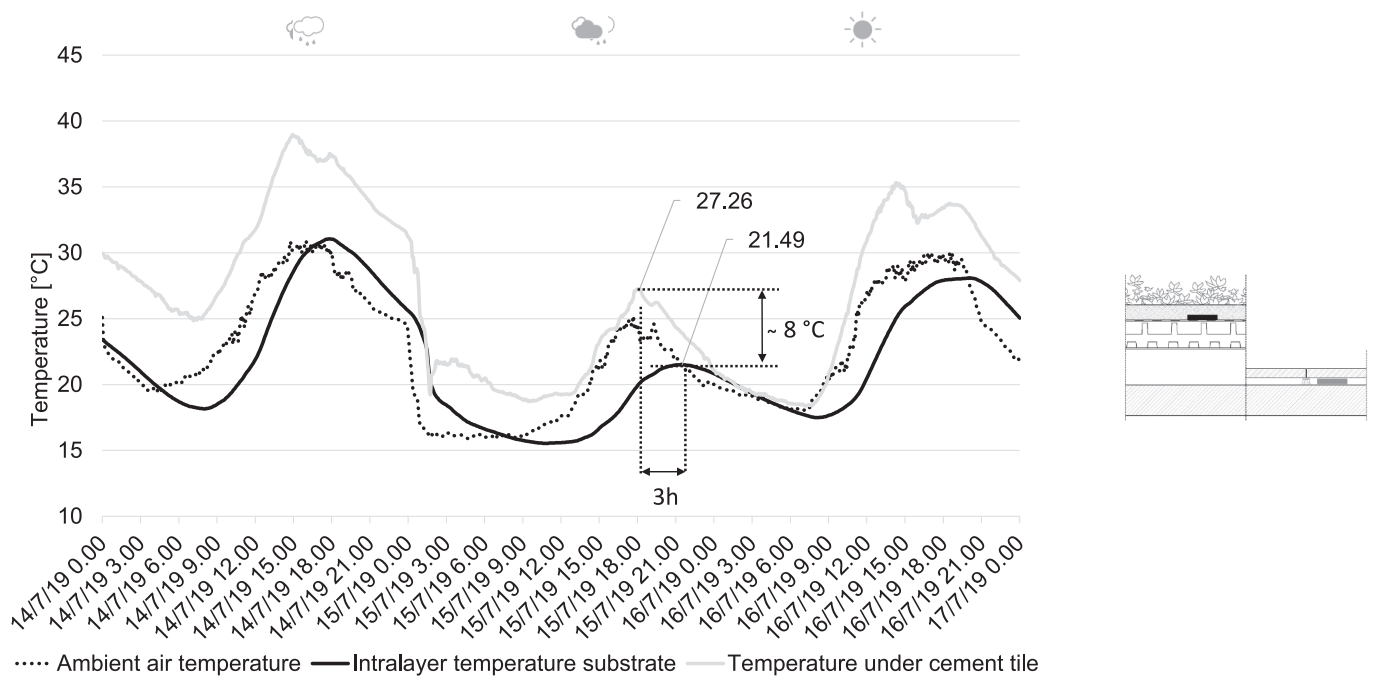


Fig. 12. Comparison of the substrate’s intralayer temperatures and the temperatures under the cement tiles for three days period, between 14th and 16th of July 2019.

section, the interpretation of the key findings is provided, discussing the implication of the results and its limitations. The section ends with avenues and recommendations for future research. Our experimental monitoring campaign to analyse the summer hygrothermal performances of a lightweight extensive green roof in comparison with a traditional horizontal roof finished with cement tiles showed coherent results with the existing literature. The results of the study can be summarised in the following key points: (i) the temperature of the vegetative layer presents a lower temperature concerning the surface

cement tile surface. The difference increases according to the water content of the ground. In detail, the temperature difference between the green surface and the cement coating after a previous rainy event is high and about 10 °C. Instead, the two analyzed temperature profile after a series of hot and sunny days are comparable with a recorded temperature difference, collected during the hottest hour of the day, between 3 and 5 °C; (ii) As expected, during a rainy day, the soil and the green layer contributes to increasing the related air humidity thanks to the water content of the green roof. During typical summer days characterized by

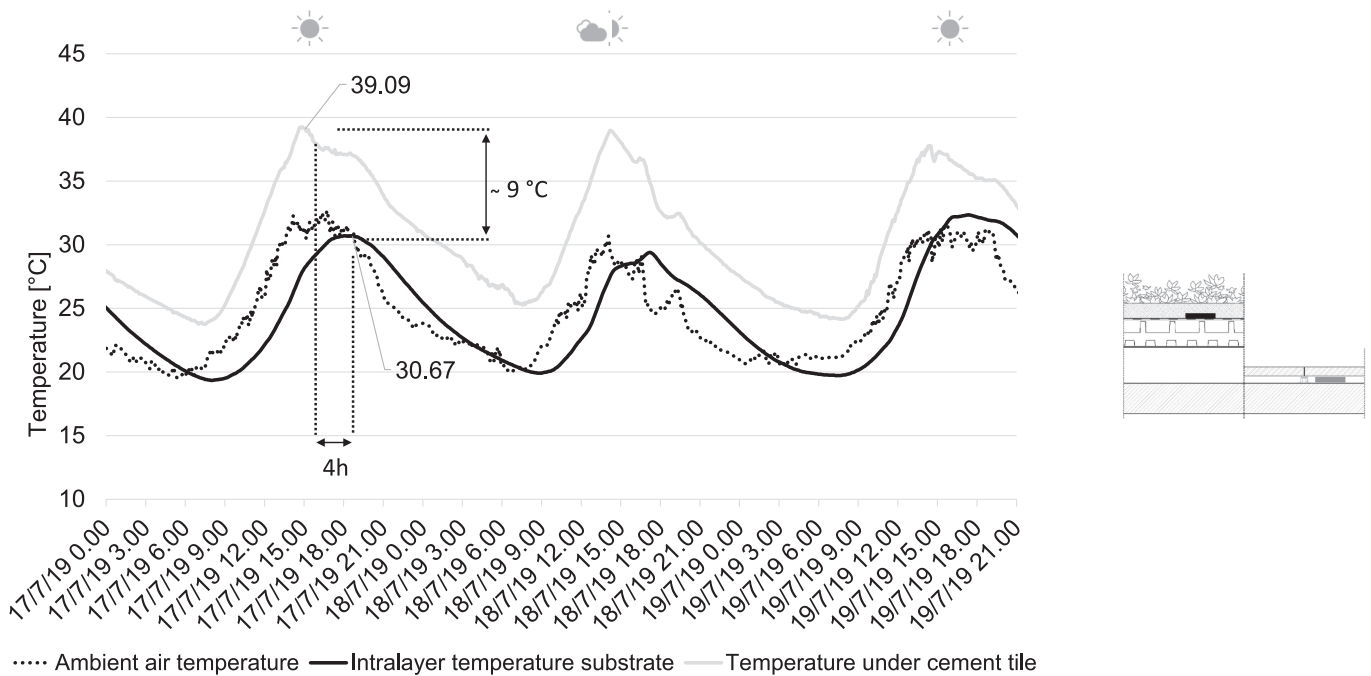


Fig. 13. Comparison of the substrate’s intralayer temperatures and the temperatures under the cement tiles for three days period, between 17th and 19th of July 2019.

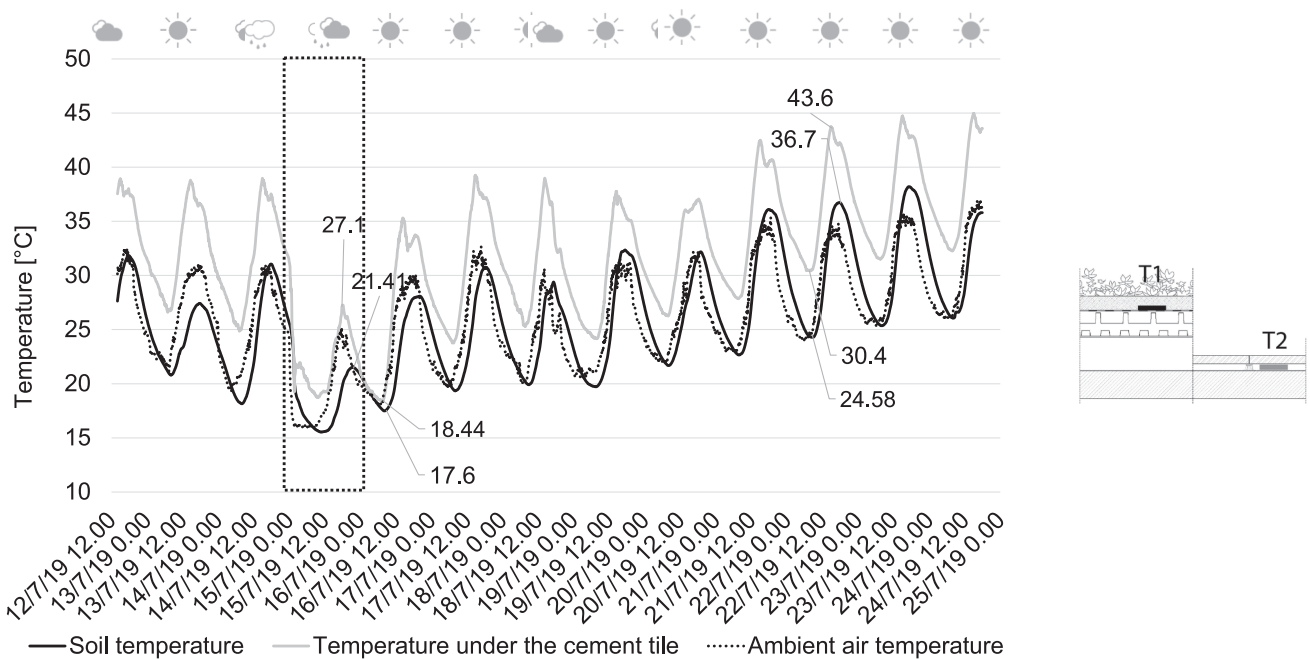


Fig. 14. Temperature difference between the ground layer and the surface temperature under the cement tiles (T1-T2). The data refers to the whole monitoring campaign.

high solar radiation and air temperature, the evapotranspiration of the green layer increase resulting in more water content of the air above the vegetative level of about 4–8 % (iii) the temperature registered at 8 cm depth of the green roof demonstrate the ability of the soil layer to shift and attenuate the temperature levels, the attenuation potential is greater the higher the ground water content is; (iv) the thermal inertia of the soil allow a temperature reduction at the ground substrate level (at 8 cm depth) of about 9–10 °C during sunny days respect to the other case. This study also provides insights from the technical point of view in using the extensive green roof technology for building renovation. The real case

study application highlights the feasibility of the installation process on a multi-layered dry building increasing the aesthetics and functionality of the roof. Moreover, the application of lightweight prefabricated technology components speeds up the renovation intervention, which lasted 14 working days (2 m²/day). Despite the insight offered by this study, some limitations should be considered. The limited number of measuring points, due mainly to the limited dimension of the sample, reduce the depth of the analysis, leading to a less comprehensive assessment of the green roof’s performances that will be further investigated on the living laboratory.

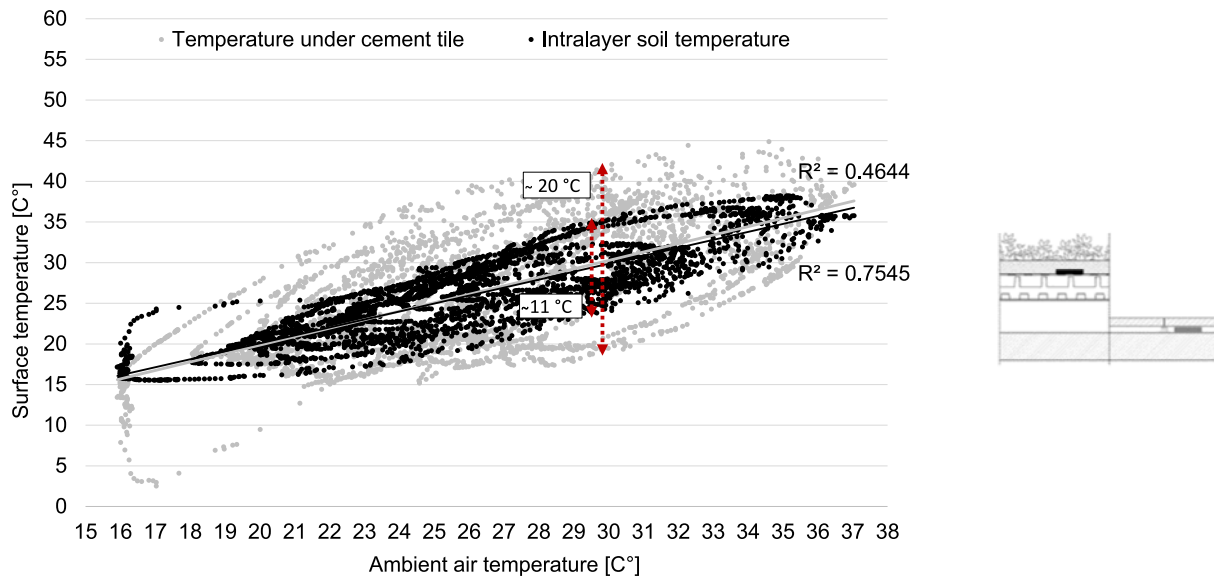


Fig. 15. Scatter plot of the intralayer ground temperatures and temperatures under the cement tile versus ambient air temperature. The data refers to the whole monitoring campaign.

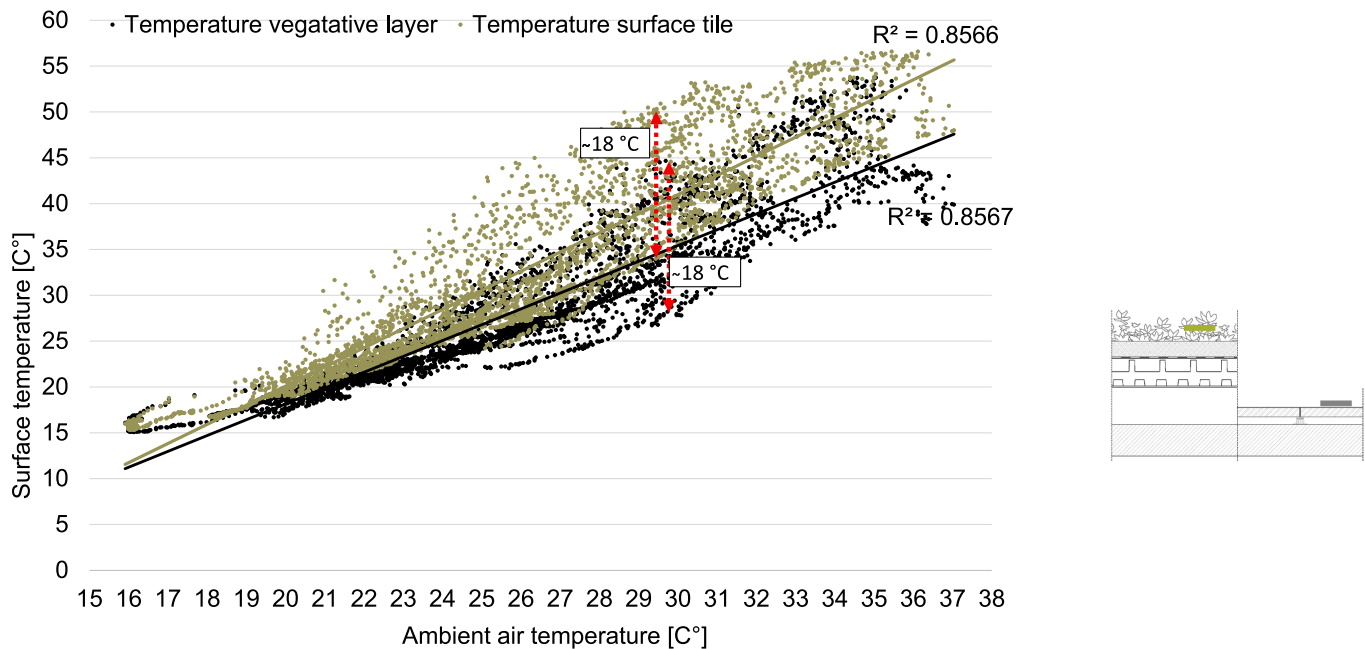


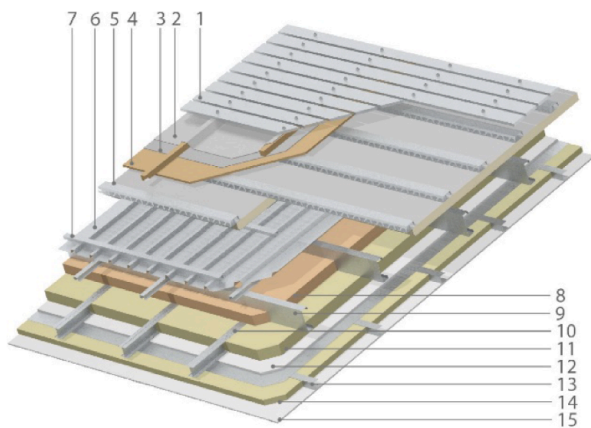
Fig. 16. Scatter plot of the vegetative ground temperature and the superficial temperature of the cement tile versus ambient air temperature. The data refers to the whole monitoring campaign.

6. Conclusions

Considering the urgent global issues, such as Urban Heat Island and air pollution, the European Union has expressed the need for forward-thinking strategies towards the growth of the UHI's effect and the levels of air pollution. Towards comfort increasing inside the urban environment, the need for mitigation strategies to improve environmental conditions outside and inside the buildings is becoming a priority. Among others, the scientific community recognises the potential of Nature Based Solutions to offer multiple benefits and contribute to reducing carbon emissions. In this context, the green roof can be considered a valid mitigation strategy in the already-started Renovation Wave scenario.

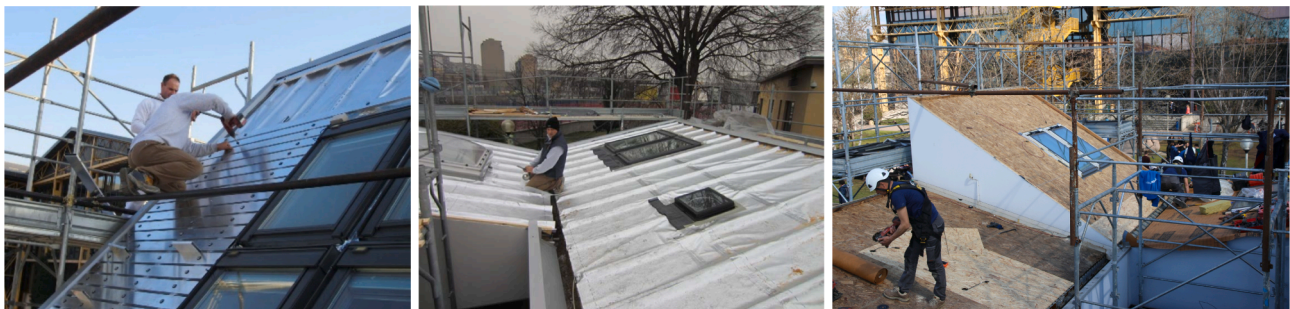
The presented work contributes to the existing literature showing the

feasibility of the green roof technology in existing buildings without limiting the study to the experimental sample test measurement. In fact, the novelty of the research relies on the case study application demonstrating and disseminating how green roof technology can be integrated into real-world scenarios for the construction industry, focusing on building renovation interventions boosting the European Renovation Wave policy. This study confirms the potential of the rising industrialized and lightweight extensive green roof technology analyzing the hygrothermal performances in comparison with a traditional horizontal roof with cement tiles and providing an application of the technology to renovate the roof of a living laboratory. This study being the first step, a future study will be carried out on the green roof installed in the living laboratory. To provide comprehensive results comparing green roof performances between different seasons, a long-term monitoring will be



1. Raw aluminium staves, fastened with stainless steel screws;
2. Transpiring, waterproof and heat-reflecting layer;
3. Transpiring and waterproof layer;
4. Oriented strand board (OSB), 15 mm;
5. Expanded polyurethane panel with ventilation profile, 60 mm;
6. Corrugated galvanized steel sheet (h. 30 mm, thk. 8/10 mm);
7. Bent steel profiles to lift the corrugated sheet (h. 25 mm);
8. Wood wool insulation type Celenit N75, thk. 75 mm;
9. C-shaped profiles made of bent steel (h. 160 mm);
10. Lightweight steel substructure for the self-supporting ceiling;
11. Rockwool panels, density = 40 Kg/m³, thk. 80 mm;
12. Plasterboard, thk.12,5 mm, with aluminium vapour barrier;
13. Lightweight steel substructure for ceiling (50x50 mm);
14. Sound absorbing layer in mineral wool felt, thk. 40 mm;
15. Perforated plasterboard, thk. 12,5 mm.

Fig. 17. Test facility building's roof layering. The overall construction is based on dry assembled lightweight technology.



a)

b)

c)

Fig. 18. Removal of the original external layers: a) Raw aluminium staves, fastened with stainless steel screws; b) Transpiring, waterproof and heat-reflecting layer; c) Transpiring waterproof layer.

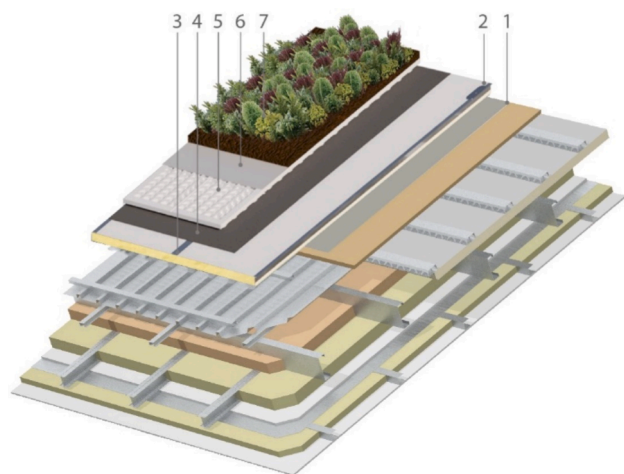
conducted including measurements. Moreover, one of the purposes of the following study is to evaluate and quantify how the green roof technology contributes to the interior comfort conditions when integrated into the existing energy-efficient envelope of the living laboratory. The study will support in clarifying how the high thermal resistance roof, combined with the thermal mass provided by the ground substrate, contributes to the indoor comfort user perception. The results of the study might be used in future research to compare or calibrate micro-climate simulation-based models of the dense build environment, where the green roof technology is applied as a promising UHI mitigation measure.

Funding

This research did not receive any specific grant from funding agencies in the public, commercial, or not-for-profit sectors.

CRediT authorship contribution statement

Graziano Salvalai: Conceptualization, Data curation, Investigation, Methodology, Supervision, Writing – original draft, Writing – review & editing. **Grazia Marrone:** Formal analysis, Data curation, Visualization, Writing – original draft, Writing – review & editing. **Marta Maria Sesana:** Formal analysis, Writing – original draft, Writing – review & editing. **Marco Imperadori:** Conceptualization, Supervision.



(ii) Placement of the sandwich panel layer:

1. Transpiring and waterproof membrane;
2. Polyurethane sandwich panel, thickness 40 mm;
3. Application of pontage band on panel's joints;

(iii) Placement of the lightweight extensive green roof system:

4. Placement of a waterproof and root barrier membrane;
 5. Placement of the drainage and water storage element, 47 mm;
 6. Placement of stabilizing geotextile and soil retention geocells;
 7. Placement of volcanic aggregate mix and ground cover plants;
- and vegetation layer installation and completion.

Fig. 19. Schematisation of the lightweight green roof system installation. (For interpretation of the references to colour in this figure legend, the reader is referred to the web version of this article.)



a)

b)

c)

Fig. 20. Schematisation and pictures of the main installation phases of the lightweight green roof system: a) Placement of stabilizing geotextile and soil retention geocells; b) Placement of volcanic aggregate mix and ground cover plants; c) Completed green roof. (For interpretation of the references to colour in this figure legend, the reader is referred to the web version of this article.)

Declaration of Competing Interest

The authors declare that they have no known competing financial interests or personal relationships that could have appeared to influence the work reported in this paper.

Data availability

The data that has been used is confidential.

Acknowledgements

The authors would like to thank Daku Italy srl for providing the extensive green roof sample used for the monitoring campaign. We thank Isopan spa and Daku Italy srl for the collaboration in the case study development by providing the materials for the renovation case study example.

References

- [1] European Union. Directive (EU) 2018/844 of the European Parliament and of the Council of 30 May 2018 amending Directive 2010/31/EU on the energy performance of buildings and Directive 2012/27/EU on energy efficiency. 2018. <https://eur-lex.europa.eu/legal-content/EN/TXT/?uri=uriserv%3AOJ.L.2018.156.01.0075.01.ENG>.
- [2] C. Sarrat, A. Lemonsu, V. Masson, D. Guedalia, Impact of urban heat island on regional atmospheric pollution, *Atmos. Environ.* 40 (2006) 1743–1758, <https://doi.org/10.1016/j.atmosenv.2005.11.037>.
- [3] M. Baccini, A. Biggeri, G. Accetta, T. Kosatsky, K. Katsouyanni, A. Analitis, H. R. Anderson, L. Bisanti, D. D'ippoliti, J. Danova, B. Forsberg, S. Medina, A. Paldy, D. Rabczenko, C. Schindler, P. Michelozzi, Heat effects on mortality in 15 European cities, *Epidemiology* 19 (2008) 711–719, <https://doi.org/10.1097/EDE.0b013e318176bfcd>.
- [4] M. Santamouris, D.N. Asimakopoulos, V.D. Assimakopoulos, N. Chrisomallidou, N. Klitsikas, D. Mangold, P. Michel, M. Santamouris, A. Tsangrassoulis, *Energy and Climate in the Urban Built Environment* (2013), <https://doi.org/10.4324/9781315073774>.
- [5] M. Santamouris, Heat island research in Europe: the state of the art, *Adv. Build. Energy Res.* 1 (2007), <https://doi.org/10.1080/17512549.2007.9687272>.
- [6] European Union (EU), Directive 2008/50/EC, Off. J. Eur. Union. L 152 (2008).
- [7] T. Croeser, G. Garrard, R. Sharma, A. Ossola, S. Bekessy, Choosing the right nature-based solutions to meet diverse urban challenges, *Urban For. Urban Green.* 65 (2021), 127337, <https://doi.org/10.1016/J.UFUG.2021.127337>.

- [8] A. Bonoli, A. Conte, M. Maglionico, I. Stojkov, Green roofs for sustainable water management in urban areas, *Environ. Eng. Manag. J.* 12 (2013) 153–156.
- [9] A. Tiwari, P. Kumar, Integrated dispersion-deposition modelling for air pollutant reduction via green infrastructure at an urban scale, *Sci. Total Environ.* 723 (2020), <https://doi.org/10.1016/j.scitotenv.2020.138078>.
- [10] U. Berardi, A. GhaffarianHoseini, A. GhaffarianHoseini, State-of-the-art analysis of the environmental benefits of green roofs, *Appl. Energy* 115 (2014) 411–428, <https://doi.org/10.1016/j.apenergy.2013.10.047>.
- [11] D. Kostadinović, M. Jovanović, V. Bakić, N. Stepanić, Mitigation of urban particulate pollution using lightweight green roof system, *Energy and Buildings*, Volume 2, 10.1016/j.enbuild.2023.113203.
- [12] W. Hong, R. Guo, H. Tang, Potential assessment and implementation strategy for roof greening in highly urbanized areas: a case study in Shenzhen, China, *Cities* 95 (2019), <https://doi.org/10.1016/j.cities.2019.102468>.
- [13] B. Barozzi, A. Bellazzi, C. Maffè, M.C. Pollastro, Measurement of thermal properties of the growing media for green roofs: assessment of a laboratory procedure and experimental results, *Buildings* 7 (2017), <https://doi.org/10.3390/buildings7040099>.
- [14] J. Yang, Z.-H. Wang, F. Chen, S. Miao, M. Tewari, J.A. Voogt, S. Myint, Enhancing hydrologic modelling in the coupled weather research and forecasting-urban modelling system, *Boundary-Layer Meteorol.* 155 (2015) 87–109, <https://doi.org/10.1007/s10546-014-9991-6>.
- [15] A.L.S. Chan, T.T. Chow, Energy and economic performance of green roof system under future climatic conditions in Hong Kong, *Energy Buildings* 64 (2013) 182–198, <https://doi.org/10.1016/j.enbuild.2013.05.015>.
- [16] M. Shaterabadi, H. Mehrjerdi, N. Amiri, M. Ahmadi Jirdehi, A. Iqbal, Green roof positive impact on changing a Plus-ZEB to drastic Plus-ZEB: the multi-objective energy planning and audit in real condition outlook, *Energy Build.* 287 (2023) 112983.
- [17] C. de Munck, A. Lemonsu, V. Masson, J. Le Bras, M. Bonhomme, Evaluating the impacts of greening scenarios on thermal comfort and energy and water consumptions for adapting Paris city to climate change, *Urban Clim.* 23 (2018) 260–286, <https://doi.org/10.1016/j.uclim.2017.01.003>.
- [18] T. Momose, J. Lundholm, Use of a thermo-module as a soil heat flux sensor: applications in the evaluation of extensive green roof thermal performance, *Energy Build.* 231 (2021), <https://doi.org/10.1016/j.enbuild.2020.110562>.
- [19] SeyedehNiloufar Mousavi, M. Gheibi, S. Wacławek, K. Behzadian, A novel smart framework for optimal design of green roofs in buildings conforming with energy conservation and thermal comfort, *Energy Build.* 291 (2023) 113111.
- [20] M. Abuseif, E. Jamei, H.-W. Chau, Simulation-based study on the role of green roof settings on energy demand reduction in seven Australian climate zones, *Energy Build.* 286 (2023) 112938.
- [21] X. Zheng, Z. Yang, J. Yang, M. Tang, C. Feng, An experimental study on the thermal and energy performance of self-sustaining green roofs under severe drought conditions in summer, *Energy Build.* 261 (2022) 111953.
- [22] P. Bevilacqua, D. Mazzeo, R. Bruno, N. Arcuri, Experimental investigation of the thermal performances of an extensive green roof in the Mediterranean area, *Energy Build.* 122 (2016) 63–79, <https://doi.org/10.1016/j.enbuild.2016.03.062>.
- [23] Y. Kaluarachchi, Potential advantages in combining smart and green infrastructure over silo approaches for future cities, *Front. Eng. Manag.* 8 (2021) 98–108, <https://doi.org/10.1007/s42524-020-0136-y>.
- [24] E. Cristiano, R. Deidda, F. Viola, The role of green roofs in urban Water-Energy-Food-Ecosystem nexus: a review, *Sci. Total Environ.* 756 (2021), 143876, <https://doi.org/10.1016/j.scitotenv.2020.143876>.
- [25] L. Cirrincione, M. La Gennusa, G. Peri, G. Rizzo, G. Scaccianoce, G. Sorrentino, S. Aprile, Green roofs as effective tools for improving the indoor comfort levels of buildings—an application to a case study in sicily, *Appl. Sci.* 10 (3) (2020) 893.
- [26] P. Bevilacqua, The effectiveness of green roofs in reducing building energy consumptions across different climates. a summary of literature results, *Renew. Sustain. Energy Rev.* 151 (2021), <https://doi.org/10.1016/j.rser.2021.111523>.
- [27] N.P. Gallardo, E.D.L. Alves, M.S.D. Silva, F.L.N. de Sousa, B.C. Santos, Evaluation of comfort and thermal efficiency in buildings with plant surroundings: An experimental study report | Avaliação de conforto e eficiência térmica em edifícios com ambientes de plantas: Um relato de estudo experimental, *Rev. Bras. Gest. e Desenv. Reg.* 17 (2021) 365–380. 10.54399/RBGDR.V17I2.6348.
- [28] G.-y. Qiu, H.-Y. Li, Q.-T. Zhang, W. Chen, X.-J. Liang, X.-z. Li, X. ze Li, Effects of evapotranspiration on mitigation of urban temperature by vegetation and urban agriculture, *J. Integr. Agric.* 12 (8) (2013) 1307–1315.
- [29] P. La Roche, U. Berardi, Comfort and energy savings with active green roofs, *Energy Build.* 82 (2014) 492–504, <https://doi.org/10.1016/j.enbuild.2014.07.055>.
- [30] M. Razzaghmanesh, S. Beecham, The hydrological behaviour of extensive and intensive green roofs in a dry climate, *Sci. Total Environ.* 499 (2014) 284–296, <https://doi.org/10.1016/j.scitotenv.2014.08.046>.
- [31] L. Kleerekoper, M. Van Esch, T.B. Salcedo, How to make a city climate-proof, addressing the urban heat island effect, *Resour. Conserv. Recycl.* 64 (2012), <https://doi.org/10.1016/j.resconrec.2011.06.004>.
- [32] D. Gößner, M. Mohri, J.J. Krespach, Evapotranspiration measurements and assessment of driving factors: a comparison of different green roof systems during summer in Germany, *Land* 10 (2021), <https://doi.org/10.3390/land10121334>.
- [33] M.F. Chow, M.F.A. Bakar, J.K. Wong, L. Ling, Evapotranspiration measurement and estimation of crop coefficient for native plant species of green roof in the tropics, *Water (switzerland)* 13 (2021), <https://doi.org/10.3390/w13121669>.
- [34] A.M. Coutts, E. Daly, J. Beringer, N.J. Tapper, Assessing practical measures to reduce urban heat: green and cool roofs, *Build. Environ.* 70 (2013) 266–276, <https://doi.org/10.1016/j.buildenv.2013.08.021>.
- [35] F. Tariku, S. Hagos, Performance of green roof installed on highly insulated roof deck and the plants' effect: an experimental study, *Build. Environ.* 221 (2022), 109337, <https://doi.org/10.1016/j.buildenv.2022.109337>.
- [36] J. Coma, G. Pérez, C. Solé, A. Castell, L.F. Cabeza, Thermal assessment of extensive green roofs as passive tool for energy savings in buildings, *Renew. Energy* 85 (2016) 1106–1115, <https://doi.org/10.1016/j.renene.2015.07.074>.
- [37] P. Stella, E. Personne, Effects of conventional, extensive and semi-intensive green roofs on building conductive heat fluxes and surface temperatures in winter in Paris, *Build. Environ.* 205 (2021), <https://doi.org/10.1016/j.buildenv.2021.108202>.
- [38] D. Kostadinović, M. Jovanović, V. Bakić, N. Stepanić, M. Todorović, Experimental investigation of summer thermal performance of the green roof system with mineral wool substrate, *Build. Environ.* 217 (2022), 109061, <https://doi.org/10.1016/j.buildenv.2022.109061>.
- [39] V. Jelínková, M. Dohnal, T. Píček, A green roof segment for monitoring the hydrological and thermal behaviour of anthropogenic soil systems, *Soil Water Res.* 10 (2015), <https://doi.org/10.17221/17/2015-SWR>.
- [40] D.V. López-Silva, R. Méndez-Alonso, D. Saucedo-Carvajal, E. Sigala-Meza, I. Zavala-Guillén, Experimental comparison of two extensive green roof designs in Northwest Mexico, *Build. Environ.* 226 (2022), 109722.
- [41] J. Heusinger, S. Weber, Comparative microclimate and dewfall measurements at an urban green roof versus bitumen roof, *Build. Environ.* 92 (2015), <https://doi.org/10.1016/j.buildenv.2015.06.002>.
- [42] M. Maiolo, B. Pirouz, R. Bruno, S.A. Palermo, N. Arcuri, P. Piro, The role of the extensive green roofs on decreasing building energy consumption in the mediterranean climate, *Sustain.* 12 (2020), <https://doi.org/10.3390/su12010359>.
- [43] A. Solcero, F. van de Ven, M. Wang, M. Rijdsdijk, N. van de Giesen, Do green roofs cool the air? *Build. Environ.* 111 (2017) <https://doi.org/10.1016/j.buildenv.2016.10.021>.
- [44] G. Salvalai, M.M. Sesana, Experimental analysis of different insulated façade technologies in summer condition, *J. Green Build.* 14 (4) (September 2019) 77–91, <https://doi.org/10.3992/1943-4618.14.4.77>.
- [45] G. Salvalai, A. Brambilla, M. Imperadori, M.M. Sesana, Nearly Zero Energy Building renovation: from energy efficiency to environmental efficiency, a pilot case study, *Energy Build.* 166 (2018) 271–283, <https://doi.org/10.1016/j.enbuild.2018.02.002>.
- [46] G. Salvalai, M.M. Sesana, D. Brutti, M. Imperadori, Design and performance analysis of a lightweight flexible nZEB, *Sustainability.* 12 (15) (2020) 5986, <https://doi.org/10.3390/su12155986>.
- [47] S. Cascone, J. Coma, A. Gagliano, G. Pérez, The evapotranspiration process in green roofs: a review, *Build. Environ.* 147 (2019) 337–355, <https://doi.org/10.1016/j.buildenv.2018.10.024>.